Vibrational Spectra and Force Constants of Symmetric Tops VL [1]

Spin Flip Raman Laser Spectra and Rotational Analysis of $(\nu_1 + \nu_2)$ of CF_3Cl and CF_3Br

M. K. Haj-Abdallah *, H. Pascher, and H. G. Häfele
Physikalisches Institut, Universität Würzburg

A. Ruoff and H. Essig
Sektion Schwingungsspektroskopie, Universität Ulm

Z. Naturforsch. **40 a**, 233–238 (1985); received December 6, 1984

The IR spectra of gaseous CF_3Cl and CF_3Br with natural isotopic abundances have been investigated in the region 1830–1900 cm^{-1} with a resolution of 0.01 cm^{-1} or better using a Q-switched spin-flip Raman laser (SFRL). Both J and K structure of the parallel band $(\nu_1 + \nu_2)$ have been resolved partly for both isotopomers of CF_3Cl and CF_3Br, respectively. The analysis has been performed by the usual least squares method. Additionally the J clusters of some hot bands have been observed and analyzed.

1. Introduction

Recently the IR spectra of CF_3Cl and CF_3Br have been the subject of renewed interest. The spectrum of ν_1 of both molecules has been recorded with a resolution of 0.0015 cm^{-1} (CF_3Cl) [2] and 0.015 cm^{-1} (CF_3Br) [3]. All other fundamentals and many overtones and combination bands have been studied with a resolution of 0.04 cm^{-1} [4–7]. Since the first observation of stimulated spin-flip Raman scattering, spin-flip Raman lasers (SFRL) have often been used as narrow-band IR radiation sources with good tuning characteristics and small linewidths. Using a Q-switched CO laser as a pump, SFRL works in the 5.3 µm region, the linewidth being a few hundred MHz. Since the combination band $(\nu_1 + \nu_2)$ of both CF_3Cl and CF_3Br falls in this region (1889 and 1844 cm^{-1}, respectively) it seemed desirable to investigate this band with a SFRL to obtain additional information on the molecular constants of the state $v_1 = v_2 = 1$. In this contribution we deal with the SFRL spectra of $(\nu_1 + \nu_2)$ of CF_3Cl and CF_3Br with natural isotopic abundances and the rovibrational analysis of this combination band and some of its hot bands.

2. SFRL Characteristics

The spin transitions in a simple parabolic band of a semiconductor lead in a magnetic field B to a Raman (Stokes) emission frequency of [9]

$$\nu_R = \nu_P - \frac{1}{h} |g^*| \mu_B B , \tag{1}$$

where ν_P is the pump frequency, g^* is the effective electron gyromagnetic ratio and μ_B is the Bohr magneton. If no mode-hopping occurs, this is also the emission frequency of SFRL. Since g^* is large in InSb (about -51 at $B = 0$), ν_R is magnetically tunable with a tuning rate of the order of 2 cm^{-1}/kG. Due to the dependence of g^* on the magnetic field and on the temperature, and due to the difficulties of measuring B with sufficient accuracy, the above equation is only accurate to within ± 0.05 cm^{-1}. Therefore secondary standard lines have to be used for calibration.

In the spin-saturated region the linewidth increases with the magnetic field. Therefore the spectra have to be recorded at low B (0.5–5 kG) and the total spectral range has to be covered by applying different pump-laser frequencies. By choosing the pump intensity sufficient to work in the spin-saturation region and by careful alignment of the beam and the sample a resolution of about 0.01 cm^{-1} in the region 1830–1850 cm^{-1} (CF_3Br) and of about 0.008 cm^{-1} in the region 1850–1900 cm^{-1} (CF_3Cl) could be achieved.

---

* Permanent address: University of Jordan, Amman, Jordan.

Reprint requests to Prof. Dr. A. Ruoff, Sektion Schwingungsspektroskopie, Universität Ulm, D-7900 Ulm, West Germany.

0340-4811 / 85 / 0300-0233 $ 01.30/0. – Please order a reprint rather than making your own copy.

3. Experimental

We used a Q-switched, low-pressure nitrogen-cooled CO laser as pump, different laser lines of which could be chosen by an intracavity grating. The pump radiation was focussed onto an InSb crystal which was immersed in pumped liquid helium and held between the poles of an electromagnet. The dimensions of this crystal were $3 \times 3 \times 10\,\mathrm{mm}^3$ and its end faces had been dielectrically coated with an antireflection layer. The Raman radiation was separated from the pump beam by a low-resolution grating monochromator. After passing the monochromator the SFRL beam was split into two parts by a CdTe beam splitter. One of the beams was focussed onto a reference detector while the other passed the 6 m absorption cell before detection. The ratio of the two signals was then recorded as a function of B. The range of operation of our SFRL was $1820-1900\,\mathrm{cm}^{-1}$. The cell was filled either with sample gas (5−20 mbar) or with mixtures of sample gas (5−10 mbar) and the calibration gas (5−15 mbar). For this purpose we used N_2O [10] and NO [11]. The spectra were calibrated using a least squares fit. The absolute accuracy of our CF_3Cl/CF_3Br lines is $\pm\,0.003\,\mathrm{cm}^{-1}$ or better.

4. Spectra and Their Analysis

4.1. General

CF_3Cl and CF_3Br are prolate symmetric top molecules giving rise to parallel or perpendicular bands in the infrared. Natural CF_3Cl consists mainly of the two isotopomers $^{12}CF_3{}^{35}Cl$ and $^{12}CF_3{}^{37}Cl$ with the abundances 74.6% and 24.3%, respectively. Henceforth these isotopomers are abbreviated as (35) and (37). Natural CF_3Br is mainly composed of the two isotopomers $^{12}CF_3{}^{79}Br$ (49.9%) and $^{12}CF_3{}^{81}Br$ (49.0%), henceforth designated as (79) and (81), respectively. The ground state constants of these isotopomers are summarized in Table 1. B_0, D_J^0 and D_{JK}^0 have been determined by MW spectroscopy [12, 13]. Combining B_0 with electron diffraction data [14] provides an estimate for A_0. The molecular force field in the harmonic approximation [15] is in good agreement with the observed D_J^0 and D_{JK}^0 values and thus should give a fair estimate of D_K^0.

$(\nu_1 + \nu_2)$ is a parallel band for which a J spacing of $\sim 2B$ ($\sim 0.22\,\mathrm{cm}^{-1}$ for CF_3Cl and $\sim 0.14\,\mathrm{cm}^{-1}$ for CF_3Br) is expected to occur. The K structure of these J clusters and of the Q branch should be much narrower. For CF_3Cl (CF_3Br) the term $[(A' - A'') - (B' - B'')]$ is expected to be about $2 \times 10^{-4}\,\mathrm{cm}^{-1}$ ($-3 \times 10^{-4}\,\mathrm{cm}^{-1}$) for $(\nu_1 + \nu_2)$ which means that with our SFRL the K components should be resolved for $K > 9$.

The bands were analyzed employing the usual polynomial method for those bands which showed clustered or masked K structure taking

$$\nu_m^{\mathrm{P,R}} = A + Bm + Cm^2 + Dm^3 + Em^4\,, \qquad (2)$$

where $m = J + 1, -J$ for $\Delta J = +1, -1$, respectively, and

$$\begin{aligned} A &= \nu_0 + [(A' - A'') - (B' - B'')]\,K^2 - (D_K' - D_K'')\,K^4 \\ B &= B' + B'' - K^2\,(D_{JK}' + D_{JK}'') \\ C &= B' - B'' - (D_J' - D_J'') \cong -\alpha^B \\ D &= -2\,(D_J' + D_J'') \\ E &= -(D_J' - D_J'')\,. \end{aligned}$$

If the K structure was resolved, we analyzed the band by a least squares fit in which the ground state constants were held fixed and the upper state parameters were refined. The upper state energy

Table 1. Ground state constants of CF_3Cl and CF_3Br.

	(35)	(37)	(79)	(81)
$A_0/10^{-1}\,\mathrm{cm}^{-1}$	1.913 [a]	1.913 [a]	1.906 [a]	1.906 [a]
$B_0/10^{-2}\,\mathrm{cm}^{-1}$	11.126346(1) [b]	10.846101(2) [b]	6.9985970(7) [d]	6.9333439(7) [d]
$D_J^0/10^{-8}\,\mathrm{cm}^{-1}$	1.8440(5) [b]	1.7593(25) [b]	0.89886(26) [d]	0.88681(30) [d]
	1.83 [c]	1.76 [c]	0.907 [c]	0.894 [c]
$D_{JK}^0/10^{-8}\,\mathrm{cm}^{-1}$	6.9297(25) [b]	6.7244(25) [b]	4.3393(10) [d]	4.2720(10) [d]
	6.92 [c]	6.72 [c]	4.40 [c]	4.33 [c]
$D_K^0/10^{-8}\,\mathrm{cm}^{-1}$	−4.12 [c]	−3.84 [c]	−0.787 [c]	−0.700 [c]

[a] See text. [b] [12]. [c] [15]. [d] [13].

was taken as

$$E' = \nu_0 + B'J(J+1) + (A'-B')K^2 - D'_J J^2 (J+1)^2 - D'_{JK} J(J+1) K^2 - D'_K K^4 . \quad (3)$$

The transition $(\nu_1+\nu_2)$ is accompanied by hot bands. The intensities of the major components relative to the cold band are expected to be as follows:

	CF_3Cl	CF_3Br
$(\nu_1+\nu_2+\nu_6)-\nu_6$	38%	46%
$(\nu_1+\nu_2+2\nu_6)-2\nu_6$	11%	17%
$(\nu_1+\nu_2+\nu_3)-\nu_3$	10%	19%
$(\nu_1+\nu_2+\nu_5)-\nu_5$	14%	15%

4.2. $(\nu_1+\nu_2)$ *of* CF_3Cl

The combination $(\nu_1+\nu_2)$ of (35) and (37) is located near 1889 cm^{-1} and shows for both isotopomers a well defined P, Q, R structure. A part of the spectrum of the P branch region is reproduced in Figure 1. The *K* structure is clearly discernible for (35) and to a less extent also for (37). The assignment was begun for (35) with a stepwise procedure. First the line positions were calculated for the $K=3n$ lines using molecular constants from the literature (Table 2, 4). By simple trial and error most of the ${}^{Q}P, R_{3n}(J)$ with $n \geqq 3$ could be assigned unambigously. The assignment of the other lines was then straightforward following the intensity alternation. The strongest peaks correspond to the unresolved transitions $K=0$ to 11 or $K=0$ to 8 in some favourable cases. No Q branch lines were assigned at this point because of the high density of lines and blending in this part of the spectrum. All assigned ${}^{Q}P, R_K(J)$ lines $(K \geqq 12)$ were then

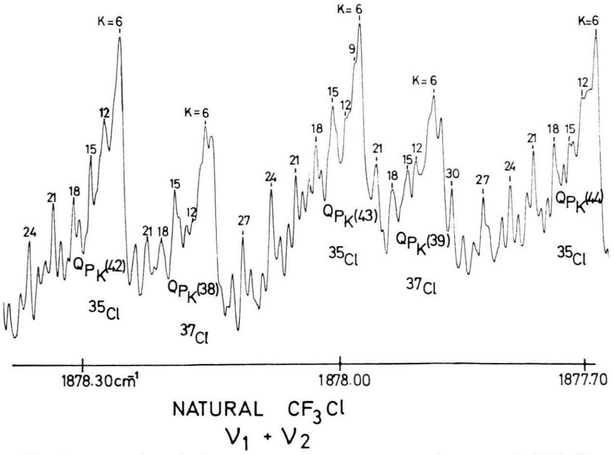

Fig. 1. Detail of the $(\nu_1+\nu_2)$ spectrum of natural CF3Cl. Assignments are given for all lines with $K=3n$ of ${}^{Q}P_K$ (44), ${}^{Q}P_K$ (43) and ${}^{Q}P_K$ (42) of $CF_3{}^{35}Cl$ and of ${}^{Q}P_K$ (39) and ${}^{Q}P_K$ (38) of $CF_3{}^{37}Cl$ respectively. The resolution is better than 0.009 cm^{-1}.

Table 2. Molecular constants of the states $v_1=v_2=1$, $v_1=1$ and $v_2=1$ of CF_3Cl. (Numbers in parentheses are one standard deviation in the last digit.)

	$v_1=v_2=1$	$v_1=1$	$v_2=1$
(35)			
ν_0/cm^{-1}	1888.9103(3)^{a} 1888.921^{c,g,h}	1108.3553(1)^{b} 1108.362(7)^{c,g,d}	783.363^{c,g,h}
$(A'-A'')/10^{-4}\ cm^{-1}$	−5.673(8)^{a}	−3.8061(41)^{b}	−1.5^{c,d}
$(B'-B'')/10^{-4}\ cm^{-1}$	−7.659(1)^{a} −7.636^{c,g}	−5.687(2)^{b} −5.716^{c,g}	−1.687(41)^{c,g}
$(D'_J-D''_J)/10^{-8}\ cm^{-1}$	0^{a,e}	0.002(14)^{b}	
$(D'_{JK}-D''_{JK})/10^{-8}\ cm^{-1}$	0.34(2)^{a}	0.10(4)^{b}	
$(D'_K-D''_K)/10^{-8}\ cm^{-1}$	−1.24(6)^{a}	0^{b,e}	
$\sigma/10^{-3}\ cm^{-1}$	1.9^{a}	2.4^{b}	
(37)			
ν_0/cm^{-1}	1887.4318(5)^{a}	1108.0246(2)^{b}	782.27^{c,f}
$(A'-A'')/10^{-4}\ cm^{-1}$	−5.679(20)^{a}	−3.8322(66)^{b}	
$(B'-B'')/10^{-4}\ cm^{-1}$	−7.408(3)^{a}	−5.490(4)^{b}	
$(D'_J-D''_J)/10^{-8}\ cm^{-1}$	0^{a,e}	−0.24(2)^{b}	
$(D'_{JK}-D''_{JK})/10^{-8}\ cm^{-1}$	0.32(7)^{a}	0.43(6)^{b}	
$(D'_K-D''_K)/10^{-8}\ cm^{-1}$	−1.15^{a,e}	0^{be}	
$\sigma/10^{-3}\ cm^{-1}$	1.9^{a}	3^{b}	

[a] This work. [b] [2]. [c] [4, 5]. [d] Band contour simulation. [e] Constrained, see text. [f] Edge of the Q branch. [g] Polynomial fit. [h] Calculated from polynomial coefficient *A* assuming $K=6$.

subjected to a least squares fit yielding improved upper state parameters. These constants allowed the prediction of additional lines, especially of ${}^{Q}Q_K\,(J)$ lines, and further assignments were obtained. Band contour simulations revealed that for CF_3Cl the maxima of the strongest peaks correspond roughly to $K = 6$. These peaks were treated as $K = 6$ lines but given a lower weight in the final fit. In the course of the calculations it became obvious that the very small term $(D'_J - D''_J)$ was statistically meaningless. Consequently it was constrained to zero. Finally we were able to assign 1164 ${}^{Q}P, Q, R_K\,(J)$ lines ($6 \leqq K \leqq 39$; $6 \leqq J \leqq 70$). This assignment was checked and confirmed by the usual method of ground state combination differences [16] yielding for (35) $B_0 = 0.111253(6)\ \mathrm{cm^{-1}}$, $D_J^0 = 1.81\,(10) \times 10^{-8}\ \mathrm{cm^{-1}}$ and $D_{JK}^0 = 5.2\,(10) \times 10^{-8}\ \mathrm{cm^{-1}}$ which are in good agreement with the MW results (Table 1). After deleting all blended lines a final least squares fit was made to determine the upper state constants. The result for (35) is given in Table 2. Lists of observed and calculated transition frequencies and correlation matrices of free parameters have been deposited as supplementary material [17].

The assignment of the lines of (37) was facilitated by the analogy with the spectrum of (35) but rendered more difficult by the lower abundance of (37). Many lines of (37) are masked by stronger features of the the other isotopomer. Thus it was only possible to detect and assign 440 ${}^{Q}P, R_K\,(J)$ lines ($6 \leqq K \leqq 33$; $7 \leqq J \leqq 79$), K being mostly a multiple of 3 [17]. The term $(D'_K - D''_K)$ of (37) was poorly defined by our data since only few transitions with $K > 24$ were measured. Therefore we assumed the ratio D'_K/D''_K to be the same for the two isotopomers. $(D'_J - D''_J)$ was constrained to zero as above. The results of our final fit are reproduced in Table 2.

4.3. $(\nu_1 + \nu_2 + \nu_x) - \nu_x$ *of* CF_3Cl

Recently the hot band $(\nu_1 + \nu_2 + \nu_6) - \nu_6$ of pure (35) has been analyzed [4]. Using these results and the anharmonicity constants given in that paper we have identified sets of transitions belonging to $(\nu_1 + \nu_1 + n\,\nu_6) - n\,\nu_6$ ($n = 1, 2$) of (35). All these lines have to be assigned as the most intense transitions, i.e. as hypothetical lines ${}^{Q}P, R_K\,(J)$ with $K = 6$ [17]. No individual lines could be definitely observed. Therefore only polynomial fits were performed, the results of which are set out in Tables 4 and 5. For comparison the corresponding polynomial coefficients are given for $(\nu_1 + \nu_2)$, ν_1 and ν_2. No further hot bands were identified with certainty.

4.4. $(\nu_1 + \nu_2)$ *of* CF_3Br

The P, Q, R structure of this band located at $1844\ \mathrm{cm^{-1}}$ is well discernible. The identification of the lines is more difficult than in CF_3Cl for two reasons:

Table 3. Molecular constants of the states $v_1 = v_2 = 1$, $v_1 = 1$ and $v_2 = 1$ of CF_3Br. (Numbers in parentheses are one standard deviation in the last digit.)

	$v_1 = v_2 = 1$	$v_1 = 1$	$v_2 = 1$
(79)			
$\nu_0/\mathrm{cm^{-1}}$	$1843.719(1)^{a}$ $1843.728(10)^{e,g,h}$	$1084.765^{b,g,h}$	$762.141^{d,g,h}$
$(A' - A'')/10^{-4}\ \mathrm{cm^{-1}}$	$-5.87(4)^{a}$	$-4.4^{b,f}$ $-3.98(10)^{c}$	$-1.7(2)^{d,f}$
$(B' - B'')/10^{-4}\ \mathrm{cm^{-1}}$	$-2.958(11)^{a}$ $-3.038^{e,g}$	$-2.18(31)^{b,g}$	$-0.69^{d,g}$
$(D'_J - D''_J)/10^{-8}\ \mathrm{cm^{-1}}$	$0.10(2)^{a}$		
$\sigma/10^{-3}\ \mathrm{cm^{-1}}$	2.2^{a}		
(81)			
$\nu_0/\mathrm{cm^{-1}}$	$1843.120(1)^{a}$ $1843.2^{e,i}$	$1084.523^{b,g,h}$	$761.961^{d,g,h}$
$(A' - A'')/10^{-4}\ \mathrm{cm^{-1}}$	$-5.83(3)^{a}$	$-4.4^{b,f}$	$-1.7(2)^{d,f}$
$(B' - B'')/10^{-4}\ \mathrm{cm^{-1}}$	$-2.906(9)^{a}$	$-2.17(39)^{b}$	$-0.68^{d,g}$
$(D'_J - D''_J)/10^{-8}\ \mathrm{cm^{-1}}$	$0.05(1.4)^{a}$		
$\sigma/10^{-3}\ \mathrm{cm^{-1}}$	1.8^{a}		

[a] This work. [b] [3]. [c] [8]. [d] [6]. [e] [7]. [f] Band contour simulation. [g] Polynomial fit.
[h] Calculated from polynomial coefficients A assuming $K = 3$. [i] Edge of the Q branch.

Table 4. Coefficients of the polynomial $A + Bm + Cm^2 + Dm^3 + Em^4$ and mean deviations between observed and calculated frequencies of CF_3Cl and CF_3Br. (Numbers in parentheses are one standard deviation in the last digit.)

Molecule		A/cm^{-1}	B/cm^{-1}	$C/10^{-4} \cdot cm^{-1}$	$D/10^{-8} \cdot cm^{-1}$	$E/10^{-10} \cdot cm^{-1}$	$\sigma/10^{-3} \cdot cm^{-1}$	
$CF_3{}^{35}Cl$	ν_1	1108.373	0.221963	−5.716	−7.6		4.1	b
	ν_2	783.3632(3)	0.222350(53)	−1.687(41)	−7.4		1.1	b
	$\nu_1 + \nu_2$	1888.922(0.3)	0.221740(10)	−7.677(3)	7.3(5)	5.7(7)	2.7	a
		1888.929	0.221823	−7.636	−9.1		4.1	b
	$(\nu_1 + \nu_2 + \nu_6) - \nu_6$	1886.287(0.4)	0.22123(1)	−7.659(3)			2.9	a
		1886.297	0.221671	−7.696	−20.5		4.4	b
	$(\nu_1 + \nu_2 + 2\nu_6) - 2\nu_6$	1883.608(1)	0.22120(2)	−7.665(5)			3.6	a
$CF_3{}^{37}Cl$	$\nu_1 + \nu_2$	1887.438(0.3)	0.216170(10)	−7.401(2)	−5.8(5)		2.9	a
		1887.4						b, f
$CF_3{}^{79}Br$	ν_1	1084.763(1.5)	0.13967(19)	−2.18(3)			3.9	c
	ν_2	762.140	0.13969	−0.69			5.2	d
	$\nu_1 + \nu_2$	1843.717(1)	0.13964(2)	−2.98(1)	−4.3(5)	−6.8(14)	3.4	a
		1843.725	0.13961	−3.038			6.9	e
	$(\nu_1 + \nu_2 + \nu_6) - \nu_6$	1841.650(1)	0.13945(1)	− 3.01(1)			3.3	a
		1841.7(1)						e, f
	$(\nu_1 + \nu_2 + 2\nu_6) - 2\nu_6$	1839.586(1)	0.13919(2)	−2.99(1)			4.4	a
		1839.7(1)						e, f
	$(\nu_1 + \nu_2 + \nu_3) - \nu_3$	1846.369(2)	0.13950(2)	−2.98(1)			4.6	a
		1846.6(1)						e, f
$CF_3{}^{81}Br$	ν_1	1084.521(2)	0.13840(22)	−2.17(39)			4.7	c
	ν_2	761.960	0.13840	−0.68			5.8	d
	$\nu_1 + \nu_2$	1843.117(0.5)	0.13831(2)	−2.93(0.2)	−3.1(4)		3.2	a
		1843.2						e, f
	$(\nu_1 + \nu_2 + \nu_6) - \nu_6$	1841.061(1)	0.13820(2)	−2.92(0.3)	−4.8(7)		3.2	a
		1841.2(1)						e, f
	$(\nu_1 + \nu_2 + 2\nu_6) - 2\nu_6$	1839.023(1)	0.13782(2)	−2.91(1)			4.2	a
		1839.2(1)						e, f
	$(\nu_1 + \nu_2 + \nu_3) - \nu_3$	1845.767(1)	0.13827(2)	−2.92(1)			4.0	a
		1846.05(10)						e, f

[a] This work. [b] [4, 5]. [c] [3]. [d] [6]. [e] [7]. [f] Edge of the Q branch.

Table 5. Number of lines used for the evaluation of the polynomial coefficients (Table 4).

	(35)	(37)	(79)	(81)
$\nu_1 + \nu_2$	135	120	92	86
$(\nu_1 + \nu_2 + \nu_6) - \nu_6$	110	–	48	56
$(\nu_1 + \nu_2 + 2\nu_6) - 2\nu_6$	79	–	62	50
$(\nu_1 + \nu_2 + \nu_3) - \nu_3$	–	–	26	24

Table 6. Selected effective anharmonic constants of CF_3Cl and CF_3Br (cm^{-1}).

	(35)	(37)	(79)	(81)
x_{12}	−2.808(7) [a,d]	−2.85 [a,f]	−3.19 [a,e]	−3.36 [a,e]
	−2.807(7) [b,e]		−3.18(1) [c,e]	−3.25(5) [c,e]
$x_{16} + x_{26}$	−2.64 [a,]		−2.07 [a,e]	−2.06 [a,e]
	−2.63 [b,e]		−2.07 [c,e]	−2.05 [c,e]
$x_{13} + x_{23}$			2.65 [a,e]	2.65 [a,e]
			2.44 [c,e]	2.26 [c,e]

[a] This work. [b] [4, 5]. [c] [7].
[d] From rotational analysis including *K* structure.
[e] From polynomial coefficients *A*.
[f] From edges of the Q branches.

1. Due to the smallness of *B* and the presence of two isotopomers in nearly equal abundance the density of the *J* clusters is high compared with CF_3Cl.
2. The resolution in the region 1830 – 1850 cm^{-1} is only about 0.01 cm^{-1}, i.e. lower than for CF_3Cl.

The assignment was made in a manner similar to that described above. Starting from values predicted from known parameters (Tables 3, 4) we were able to assign the *J* clusters of both isotopomers. A band contour simulation indicated that the maxima of these *J* clusters correspond to $K = 4$. In the final fit these peaks were therefore included as $^{Q}P, R_4\ (J)$ lines and were given a lower weight. The higher *K* components are not very pronounced in the spectrum and were mostly masked by features of the other isotopomer, especially in the *R* branch. Finally 118 $^{Q}P, R_K\ (J)$ lines of (79) ($4 \leqq K \leqq 18$; $9 \leqq J \leqq 79$) and 114 $^{Q}P, R_K\ (J)$ lines of (81) ($4 \leqq K \leqq 18$; $12 \leqq J \leqq 73$) were assigned unambigously, *K* being mostly 4 [17]. Due to these low *K* values neither

$(D'_{JK} - D''_{JK})$ nor $(D'_K - D''_K)$ could be evaluated; consequently they were fixed to zero. In the final fit only ν_0, $(B' - B'')$, $(A' - A'')$ and $(D'_J - D''_J)$ were allowed to vary. The results are presented in Table 3.

4.5. $(\nu_1 + \nu_2 + \nu_x) - \nu_x$ *of* CF_3Br

Using the data of [7] and of Table 3, groups of peaks belonging to $(\nu_1 + \nu_2 + n\,\nu_6) - n\,\nu_6$ $(n = 1, 2)$ and $(\nu_1 + \nu_2 + \nu_3) - \nu_3$ were found for both isotopomers. All these peaks are the unresolved maxima of J clusters, of ^{Q}P, R$_K$ (J) lines with K approximately equal to 4 [17]. No higher K components and no lines belonging to other hot bands were identified with certainty. The results of the polynomial fit are collected in Tables 4 and 5 in which the corresponding coefficients of $(\nu_1 + \nu_2)$, ν_1 and ν_2 are given for comparison.

5. Discussion

The present study provides experimental data concerning $(\nu_1 + \nu_2)$ and some of its hot bands for (35), (37), (79) and (81). For the first time the K structure of this combination was at least partially resolved yielding molecular constants of higher quality than hitherto known for the $v_1 = v_2 = 1$ states of CF_3Cl and CF_3Br. Our results are collected in Tables 2 to 6. It is evident that the parameters for (35)/(37) and (79)/(81) show internal consistency and are in good agreement with literature values with the exception of $x_{13} + x_{23}$ of (79) and (81). The constants D'_J and D'_{JK} evaluated in this study are close to the corresponding ground state values. Contrary to this consistency, D'_K of (35) differs by about 30% from D^0_K. At the moment we cannot offer an explanation for this observation but suggest that it reflects the influence of an undetected global resonance. In contrast to ν_1 of (35) and (37) [2], the combination band shows no local perturbation. The additivity of the $\alpha^{A,B}$, according to the equation

$$(X'' - X') = \alpha_1^X + \alpha_2^X \quad (X = A, B) \tag{4}$$

is not fulfilled exactly, as has been found previously [4, 5, 7].

Spectra of pure isotopomers would yield data of better quality.

Acknowledgements

Financial support by the Deutsche Forschungsgemeinschaft and by the Fonds der Chemie is gratefully acknowledged. M. K. Haj-Abdallah wishes to thank the University of Jordan and the DAAD for making possible his stay at the University of Würzburg.

[1] H. Bürger and R. Grassow, Spectrochim. Acta, in press.
[2] S. Giorgianni, R. Visinoni, A. Gambi, S. Ghersetti, G. Restelli, and F. Cappellani, J. Mol. Spectrosc. **101,** 245 (1983); S. Giorgianni, R. Visinoni, A. Gambi, S. Ghersetti, F. Cappellani, and G. Restelli, J. Mol. Spectrosc. **104,** 40 (1984).
[3] K. Burczyk, H. Bürger, A. Ruoff, and P. Pinson, J. Mol. Spectrosc. **77,** 109 (1979).
[4] H. Bürger, K. Burczyk, R. Grassow, and A. Ruoff, J. Mol. Spectrosc. **93,** 55 (1982).
[5] R. Grassow, Dissertation, Universität Wuppertal 1983; H. Bürger and R. Grassow, Private Communication; H. Bürger, R. Grassow, and A. Ruoff, Spectrochim. Acta **39 A,** 985 (1983).
[6] K. Burczyk, H. Bürger, P. Schulz, and A. Ruoff, Z. anorg. allg. Chemie **474,** 74 (1981).
[7] H. Bürger, K. Burczyk, P. Schulz, and A. Ruoff, Spectrochim. Acta **38 A,** 627 (1982).
[8] H. Jones, F. Kohler, and H. D. Rudolph, J. Mol. Spectrosc. **63,** 205 (1976).
[9] S. R. Brueck and A. Mooradian, J.E.E.E., J. quant. Electron **10,** 634 (1974).
[10] C. Amiot and G. Guelachvili, J. Mol. Spectrosc. **59,** 171 (1976).
[11] A. Valentin, A. Henry, P. Cardinet, M. L. Le Moal, Da-Wun Chen, and K. N. Rao, J. Mol. Spectrosc. **70,** 9 (1978).
[12] J. H. Carpenter, J. D. Muse, C. E. Small, and J. G. Smith, J. Mol. Spectrosc. **93,** 286 (1982).
[13] J. H. Carpenter, J. D. Muse, and J. G. Smith, J. Chem. Soc. Faraday Trans. **78,** 139 (1982).
[14] V. Typke, M. Dakkouri, and H. Oberhammer, J. Mol. Structure **44,** 85 (1978).
[15] H. Bürger, K. Burczyk, D. Bielefeldt, H. Willner, A. Ruoff, and K. Molt, Spectrochim. Acta **35 A,** 875 (1979).
[16] W. E. Blass and T. H. Edwards, J. Mol. Spectrosc. **24,** 111 (1967).
[17] Lists of observed and calculated transition frequencies and the correlation matrices may be obtained from Fachinformationszentrum Energie-Physik-Mathematik D-7514 Eggenstein-Leopoldshafen, West Germany, on submission of the authors name, the literature reference and the registry Nr. IRD 10015.